Rock Mech. Rock Engng. (2008) 41 (1), 3–36
DOI 10.1007/s00603-007-0151-x
Printed in The Netherlands

Rock Mechanics and Rock Engineering

A Multidisciplinary Methodology for Hazard and Risk Assessment of Rock Avalanches

By

M. Castelli, C. Scavia

Politecnico di Torino – Dipartimento di Ingegneria Strutturale e Geotecnica, Torino, Italy

Received May 17, 2006; accepted March 21, 2007
Published online November 20, 2007

Summary

A quantitative procedure for hazard and risk assessment of large landslides that can develop as rock avalanches is discussed in this paper. Reference is made to the IMIRILAND project, where a multidisciplinary methodology has been developed paying particular attention to the landslide modeling process that leads to the quantification of the hazard, i.e. the prediction of the occurrence probability, the involved area and the run-out velocity. The risk assessment methodology is exemplified in the paper with reference to two cases: the Ceppo Morelli and Rosone landslides, both of which are located in the Italian Western Alps. The results of these applications show that, despite the development of sophisticated 3D numerical methods, many uncertainties still remain in the process of modeling large and complex landslides, related in particular to the definition of the probability of failure and the rheological parameters to be used for the prediction of rock mass behavior. However geo-mechanical models are found to be very valuable tools to verify, from a mechanical point of view, the assumptions introduced through the geo-structural and geo-morphological analyses concerning the volume and the kinematics of the unstable mass, and their role is fundamental for the determination of the involved area when mechanical parameters can be assumed with sufficient reliability.

Keywords: Large landslides, rock avalanches, hazard analysis, risk analysis.

1. Introduction

The concepts of landslide hazard and risk have been faced by many authors in recent years (e.g. Varnes, 1984; Einstein, 1988; Cherubini et al., 1993; Canuti and Casagli, 1994; Cruden and Fell, 1997; Berggren and Berglund, 2000). Their evaluation, however, is very difficult in the case of large landslides that can lead to catastrophic rock avalanches, i.e. very rapidly moving debris flows derived from the disintegration of a very large size failed rock mass (Pirulli, 2005). The speed reached during the run-out phase often exceeds 100 km/h, and the involved volume is commonly more than $1 \times 10^6\,m^3$.

Despite several direct and indirect impacts on human life and infrastructures, which make them a significant hazard for the exposed areas, the behavior of such phenomena is never repetitive. It is thus impossible to assess their hazard only on the basis of historical analysis of statistical data as is common practice in flood and rock fall prediction (Vengeon et al., 2001). Moreover, some mechanisms involved in this complex behavior can produce specific evolution scenarios with different impacts on the threatened elements. It is therefore essential to assess several scenarios (not only the worst case), and their potential consequences, to quantify the direct and indirect risk components in comparable terms.

For this purpose, a multidisciplinary methodology has been proposed as part of the IMIRILAND project on the basis of historical, geological (geo-morphological, geo-structural) and geo-mechanical approaches (Bonnard et al., 2004). Each of these approaches is able to provide quantitative or qualitative information on each hazard component, with different degrees of complexity (i.e. number of involved variables).

As an example a geo-morphological model is able to define different danger scenarios simply on the basis of the multi-temporal interpretation of aerial photo-

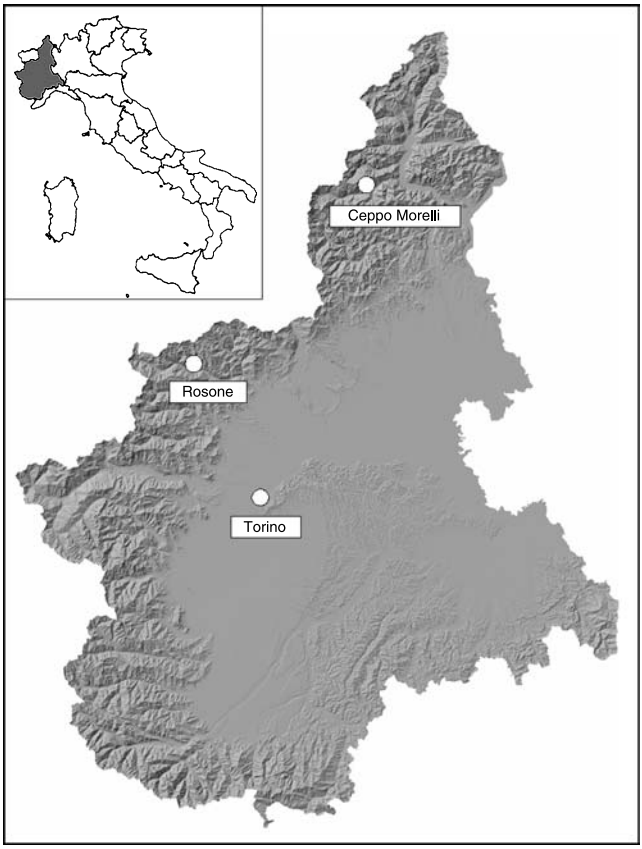

Fig. 1. Location of the Ceppo Morelli and Rosone landslides

graphs, and to indicate the involved volumes, the potentially involved area, and the relative probability of occurrence of each of them. The same can be said for the historical analysis of past events, which is able to define a frequency for different danger scenarios but also the involved volumes and the accumulation areas in qualitative terms.

However, in the case of large and complex landslides, the amount of information necessary to obtain a quantitative evaluation of the hazard components is so large that only an integrated methodology, where the results of a simple analysis supply the input to a more complex one, seems able to take into account all the features of the phenomenon.

In this paper the Quantitative Risk Assessment (QRA) methodology developed as part of the IMIRILAND project, is described by highlighting the contribution of the modeling process to the final results in terms of risk level referring to different scenarios. In particular, the available methods for the evaluation of the occurrence probability are discussed, with reference to the crucial role of this parameter in the hazard evaluation and to the great uncertainty related to its determination in the case of large landslides.

Two case studies are presented (the Rosone and Ceppo Morelli landslides, both located in the Italian Western Alps, as shown in Fig. 1), where the risk assessment methodology has been exemplified in order to show its wide applicability to different situations in different contexts.

2. The Quantitative Risk Assessment Methodology

Quantitative Risk Assessment (QRA), developed to estimate industrial risks, is a method that can be used to quantify the level of risk through a systematic analysis of the factors that contribute to the hazard and affect the severity of the consequences. The

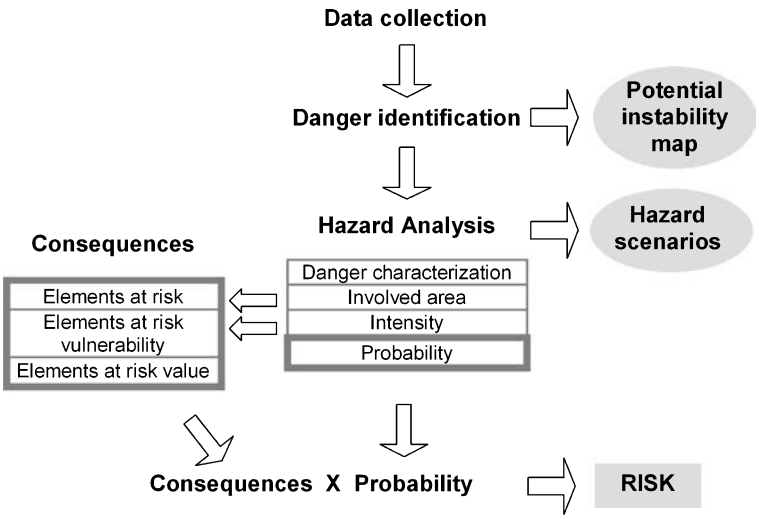

Fig. 2. Main steps in relation to a risk assessment process in the case of large landslides

following steps have been identified in the IMRILAND project for the QRA procedure in the case of large landslides (Fig. 2; for more details see Bonnard et al., 2004):

1. data-collection;
2. danger identification and characterization on the basis of collected data and field observations;
3. multidisciplinary approach to hazard analysis;
4. consequence analysis, including vulnerability analysis and value estimation of the elements at risk;
5. risk calculation, multiplying the consequences by the occurrence probability.

A crucial point of this procedure is the hazard quantification. In order to improve the hazard analyses, particular attention was paid in the project to offer as much details as possible to all its components (Fig. 2). The first component is the danger characterization, which points out the main geo-structural and geo-morphological constraints allowing the construction of geo-mechanical models and the identification of the scenarios. Once the scenarios have been identified, their hazard is given by the combination of three aspects:

a) involved area, which describes the limits of the possible evolution of the landslide;
b) process intensity, which defines the potential destructive impact of the landslide;
c) occurrence probability, i.e. the probability that a certain danger will occur in a specified period of time in a given area with a given intensity.

The quantification of each of these components is entrusted to the modeling process, which implies a necessary simplified representation of the reality (Castelli et al., 2001). Many approaches can be used for this purpose, on the basis of the available information and the data required for the analysis. In particular, in the case of complex and large phenomena, a multidisciplinary procedure should be considered, where several contributions are taken into account. In this way, a number of models are defined and an in-chain process can be built with the results of some models being used as input for some more complex ones. Geological, geo-structural, geo-morphological and geo-mechanical models are considered here, with the contribution of historical analysis and monitoring.

The analysis of the geo-mechanical behavior of a landslide is the last step of this in-chain modeling procedure. The aim of the analysis is to simulate the failure conditions, the involved volume, and the post-failure evolution of the run-out mass on the slope in quantitative terms. In particular, a quantitative assessment of involved areas and process intensities is necessary to determine the landslide consequences. The involved area allows the elements at risk to be spatially identified and the process intensity contributes to determine their vulnerability. The same need of a quantitative assessment is related to the occurrence probability, which directly contributes to define the risk, as it is multiplied by the consequences at the end of the calculation.

The quantification of the occurrence probability is very likely the most important aspect of a hazard analysis and has the aim of answering the fundamental question made by administrators: when will a certain danger scenario occur? Great attention has therefore been dedicated to this aspect, by discussing the capability of different methods to take into account the evolution in time of the parameters that influence landslide triggering and run-out (Sect. 2.1).

With regards to risk analysis, four categories are considered for the value of the elements at risk, and four risk categories are obtained: physical (asset and infrastructure value, material and construction costs), economic (interruption of economic activities), environmental (value of flora, fauna and buildings of historical and architectural importance) and social (people directly involved: evacuated, injured, or killed and people indirectly involved, e.g. hospitals unfit for use). This distinction is necessary because it is impossible to compare the value of each category of elements. The value of exposed objects can be considered by applying either monetary values (when possible), or coefficients that express their relative importance.

2.1 The Role of Modeling in the Evaluation of the Occurrence Probability

Occurrence probability can be defined as the chance, or probability, that a landslide will occur in specific areas and in specific periods of time. On the basis of this definition, two components should be considered: a temporal probability of failure (related to landslide triggering) and the probability that a failed volume could reach a given area in the valley (related to the post-failure run-out of the landslide).

A rigorous, quantitative, procedure should include the application of mechanical-probabilistic methods, taking into account the uncertainty of all the geometrical and mechanical parameters (slope geometry, shear strength, piezometric pressure, etc). Such a procedure cannot, however, be applied in the case of large landslides, because the uncertainty in the definition of these parameters is too large and it is not possible to define any reliable variability for them.

With reference to the temporal probability of failure the uncertainties are related, for example, to the geometry and the mechanical parameters that should be associated to the rock material and discontinuities, which cannot be directly measured. The effect of water, the seismic actions and the variation in time of the involved parameters are again a main source of uncertainty.

In the same way, it is possible to highlight many uncertainties in the definition of the involved areas through run-out numerical methods. The first problem is related to the unstable volume and its variation along the run-out path, which is often used as an input of the analyses. The second problem relates to the simulation of the mechanical parameters of the run-out mass and implies the choice of material rheology, or interaction among particles and damping factors, depending on the adopted method. These assumptions are usually based on bibliographic data or the back-analysis of past events, but this is still not sufficient for a reliable probabilistic prediction.

An alternative method is to take into account the relationship between the intensity of the triggering events, such as rainfall or earthquakes, and the landslide occurrence, through the use of empirical correlations or more sophisticated methods (i.e. neural network methods, Mayoraz et al., 1997). It is, however, still difficult to relate the given magnitude of a landslide phenomenon to the given intensity of the triggering factor and the lack of data often makes this approach inapplicable.

Taking into account all the described limitations, occurrence probability can be estimated using semi-quantitative methods on the basis of the historical analysis. If several historical records are available on different dangers in a studied area, where a

non-negligible hazard still exists, the historical approach appears to be suitable to obtain information related to the frequency of failure. In its simplest form, this method consists in recording the failures that occurred in the past and describing them in detail (date and type of failure, involved volume and area, location, etc.). A long representative period of recording and a sufficient amount of data are generally needed to consider all the phenomena. These results can be quantified through a systematic multi-temporal interpretation of aerial photographs which should allow the investigated area to be subdivided into ''homogeneous'' zones by using the interrelationships among the geo-morphology, geological field investigations and surface observations. This procedure has been applied to the Ceppo Morelli and Rosone landslides, as described in the following.

3. The Ceppo Morelli Landslide

The Ceppo Morelli landslide extends over the left side of the middle Anzasca valley in the Pennine Alps (Northern Piedmont, Italy), a few kilometers from the border with Switzerland (Fig. 1). Historical data indicate that it is a large and ancient rockslide, reactivated during the heavy meteorological event of October 2000. The landslide involves a massive gneissic rock mass, the overall surface is around 160000 m^2 and the estimated volume is about 5×10^6 m^3. Several rock falls with boulders of up to 300 m^3 reached the bottom of the valley in different periods, including the October 2000 event. Several boulders reached National Road 549, the only connection to the important tourist resort of Macugnaga, as well as secondary roads and seriously threatened the villages of Prequartera and Campioli, located at the bottom of the valley (Fig. 3).

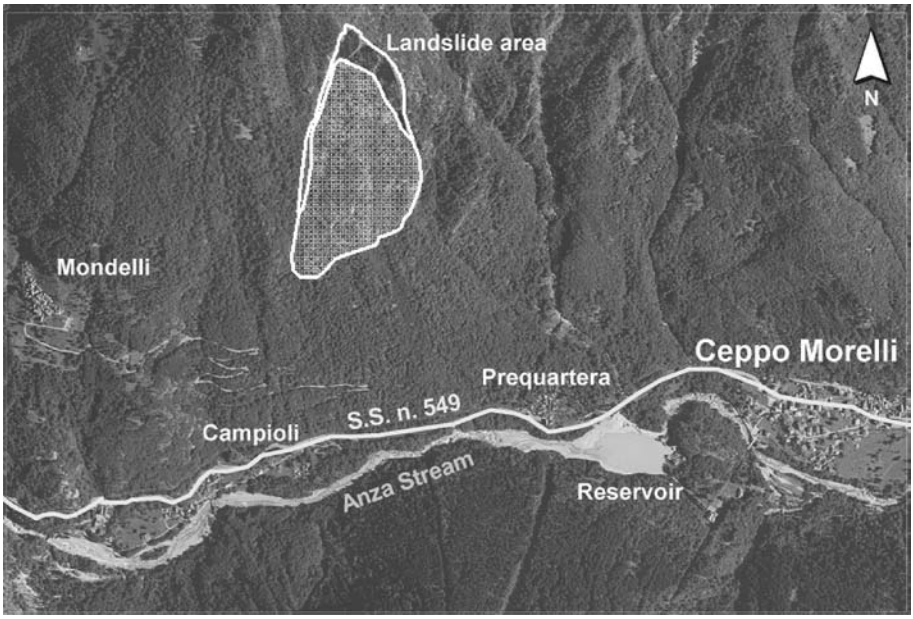

Fig. 3. Elements exposed to the Ceppo Morelli landslide

3.1 Danger Identification and Hazard Analysis

A field survey and a systematic photo-aerial analysis were conducted in order to understand the landslide behavior and to assess its hazard. The topographic and geometric features of the slope were derived from available Digital Elevation Models (DEM). The geometric and hierarchic relations among the discontinuity systems were also analyzed at a regional scale (Morelli et al., 2003) in order to derive some extrapolation rules that could offer information on the mechanical properties of the rock mass and the structural elements to be used in the geo-mechanical models. The studies and investigations carried out highlighted a rather clear morpho-dynamic and geo-structural situation in terms of recent and ancient slope evolutions. The landslide was then subdivided into three areas (Fig. 4):

A. Detachment area (upper part)

The detachment area corresponds to the upper and the western boundaries of the landslide. It presents two orthogonal discontinuity systems with NE and NW directions: the NE system, together with minor NS striking discontinuities, corresponds to

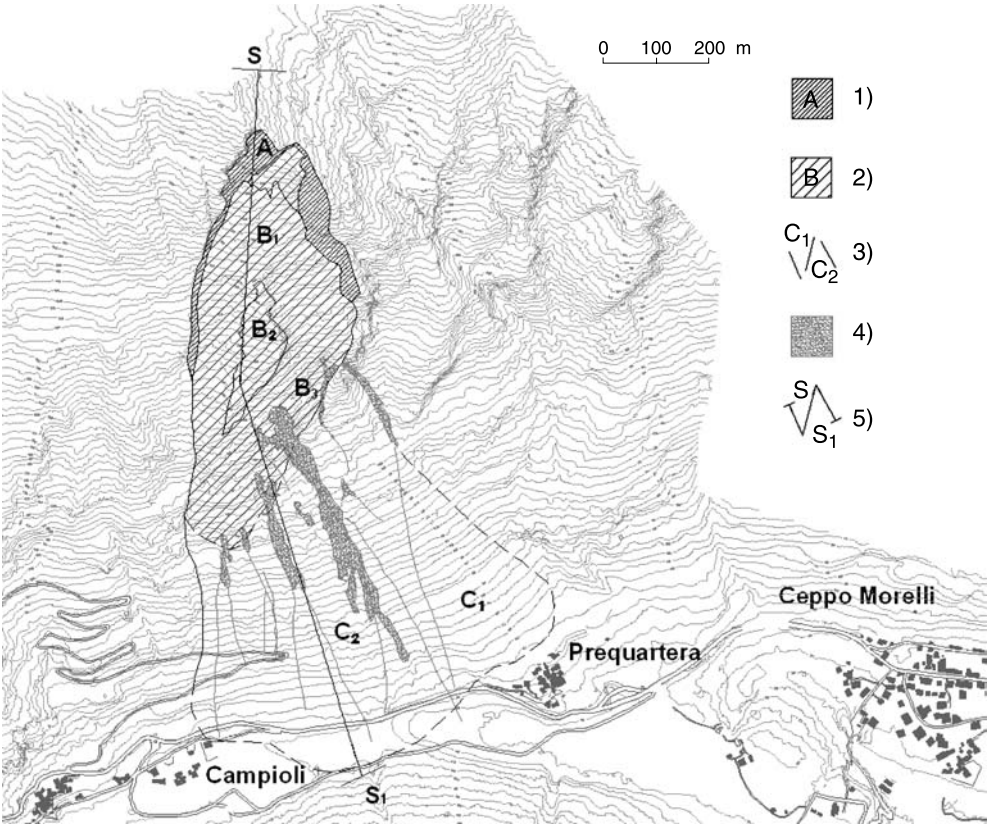

Fig. 4. Main features characterizing the Ceppo Morelli landslide: 1) detachment area; 2) rock mass translation area; 3) accumulation and landslide affected area; 4) debris flows and rock fall trajectories; 5) section S–S_1 (see Fig. 5)

the western lateral boundary of the landslide and it helped hinder the landslide movement towards the SW.

B. Rock mass translation area

This area, which corresponds to the unstable rock mass, was further subdivided into three main sectors characterized by different morpho-structural features (Fig. 4):

- sector B_1 consists of an intensively fractured rock mass and has been affected by relevant movements (up to 5 m in October 2000) towards the SSW, has occurred on a sliding surface roughly sub-parallel to the schistosity. The displacements are clearly shown by continuous opened cracks in the upper part of this sector;
- sector B_2 consists of a less fractured rock mass and preserves its original structural setting;
- sector B_3 consists of a disengaged rock mass and is separated by the B_2 sector by a clear NE striking open fracture. In the B_3 sector the inclination of the slope is greater than in the other ones (Fig. 5) and the rock shows bulging deformations and toppling. The lower boundary of the B_3 sector does not correspond to any failure surface, but it represents the morphological toe of the landslide which, although partially masked by vegetal cover, can be recognized by the alignment of some scars.

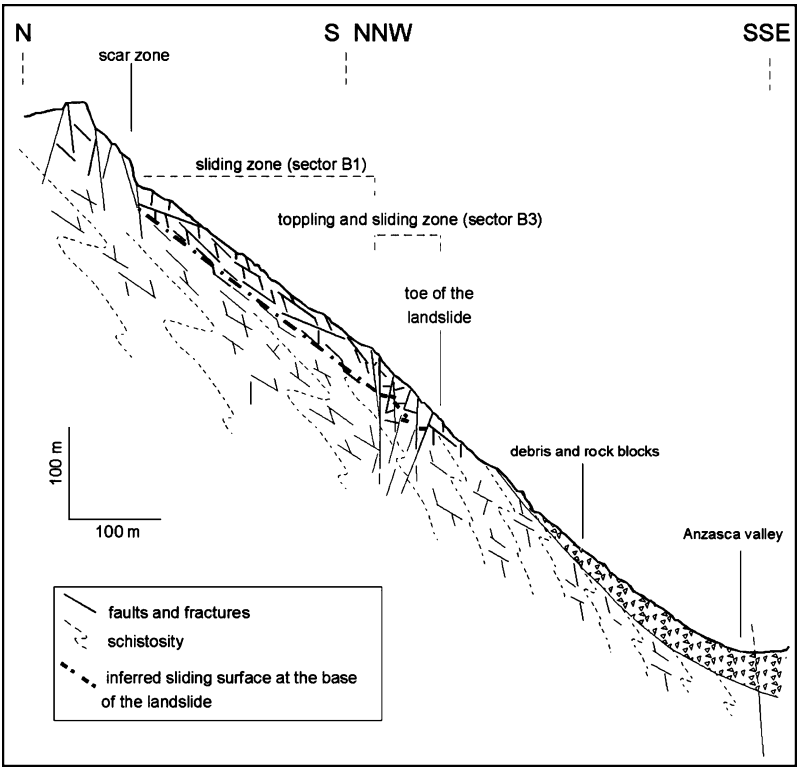

Fig. 5. Schematic cross-section of the Ceppo Morelli landslide (overall trace in Fig. 4)

C. Accumulation and landslide affected area

This fan-shaped area lies below the inferred landslide toe and is covered by debris and rock blocks, which probably fell in different periods from scars situated in sector B_3 (Fig. 4).

A schematic cross-section of the Ceppo Morelli landslide (S-S_1 in Fig. 4) is shown in Fig. 5, where the main structural elements and their cross-cutting relationships are outlined. The sliding surface in the upper part of the landslide (sliding zone) was inferred from geo-morphological data. The geometrical and structural constraints also allow the thickness of the landslide body to be inferred as a maximum (40 m) near the crown and a minimum (20 m) near the western landslide boundary.

The structural analysis was intensified in sector B_3, which was considered to be the most prone to failure. Here, the main discontinuity systems were identified (as shown in Fig. 6) in order to define the geometry and boundary conditions of the rock mass, to be used as input for the numerical analyses (for further details, see Bonnard et al., 2004):

- the schistosity and sub-parallel shear zones ZT, with a mean dip direction of 220° and a dip of 30°;
- the boundary fault on the western side (F_b), with a mean dip direction of 98° and a dip of 83°;
- the joint system F_t, with a mean dip direction of 147° and a dip of 27°;
- the joint system K_1, with a mean dip direction of 313° and a dip of 88°.

Since the October 2000 heavy rainfall event, the Ceppo Morelli landslide has been monitored using 27 topographic benchmarks. The displacements recorded from

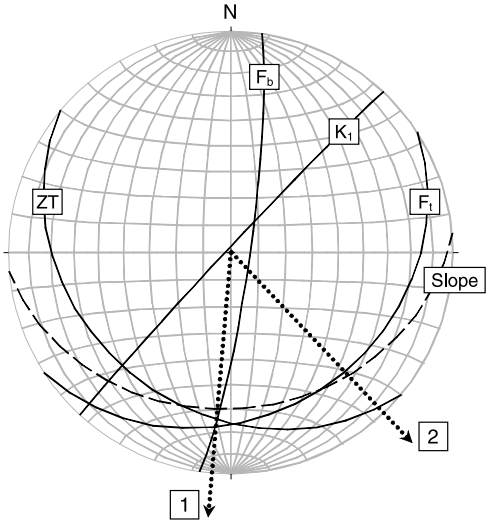

Legend

	Dip dir. (°)	Dip (°)
Slope	175	30
ZT	220	30
F_t	147	27
F_b	98	83
K_1	313	88

	Dip dir. (°)	Dip (°)
1	185	25
2	147	27

Fig. 6. Schmidt diagram (lower hemisphere) showing the mean trace of the main discontinuity systems detected in sector B_3. The kinematic mechanisms highlighted by the monitoring investigations are also shown: 1) sliding of the whole mass (western zone); 2) superficial block toppling (eastern zone)

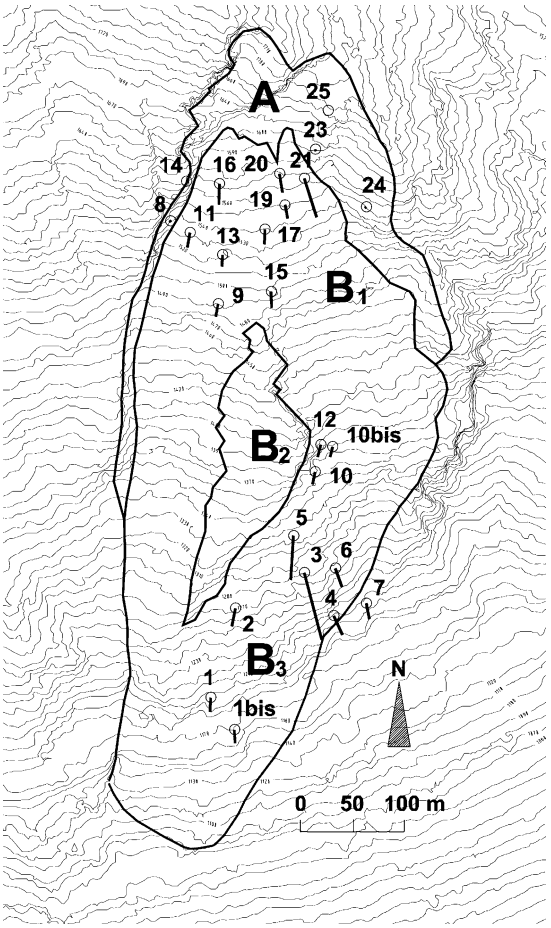

Fig. 7. Total displacement vectors measured by means of the topographic benchmarks from 5/8/2001 to 11/5/2003. The vectors are magnified by a factor of 35

August 5, 2001 to May 11, 2003 are shown in Fig. 7 and Table 1. The analysis of these results indicates that both the displacements and movement directions are rather homogeneous in the upper part of the landslide (sector B_1). The general movement direction is down-slope, i.e. SSW. This indicates that the upper part of the landslide tends to move as a single body following the line obtained from the intersection of the schistosity (which can be considered parallel to the shear zone ZT highlighted in sector B_3) with the boundary fault, F_b (direction 1 in Fig. 6). A slightly different behavior can be observed in points 17, 20 and 21, located in the eastern side of this sector. Here the direction of movement is SE (direction 2 in Fig. 6) and identifies superficial block toppling phenomena due to the intersection of the F_t system (block base) with the steeply dipping K_1 system.

Focusing attention on sector B_3, the displacement paths again show two homogeneous areas with different behavioral patterns: points 3, 4, 6 and 7 (Fig. 7) move

Table 1. Total displacements measured by means of the topographic benchmarks from 5/8/2001 to 11/5/2003 (see Fig. 7 for the point locations and displacement directions)

Point	Total displacement (mm)	Monthly average (mm/month)
1	79.07	3.77
1 bis	76.10	3.62
2	102.99	4.90
3	399.08	19.00
4	126.28	6.01
5	332.95	15.85
6	134.37	6.40
7	97.04	4.62
8	12.50	0.60
9	89.69	4.27
10	87.64	4.17
10 bis	67.23	3.20
11	7.26	0.35
12	85.08	4.05
13	94.88	4.52
14	9.14	0.44
15	111.83	5.33
16	144.07	6.86
17	93.29	4.44
19	102.93	4.90
20	141.65	6.75
21	262.83	12.52
23	40.22	1.92
24	8.74	0.42
25	–	–

with a dip direction that is close to that of the F_t system (direction 2 in Fig. 6) allowing a toppling mechanism to be assumed, whereas the ones near Sector B_2 follow a SSW direction, again as a result of the combination of the ZT system with the boundary fault F_b (direction 1 in Fig. 6), allowing a sliding mechanism to be assumed.

Two different behaviors can thus be envisaged in both sectors, the first involving a sliding of the entire mass, which was observed in the western zones, and a second superficial one involving block toppling phenomena, which was highlighted in the eastern zones, where the rock mass is more overhanging.

On the basis of the previous considerations, three different hazard scenarios are thus possible, with decreasing occurrence probability and increasing impact on land planning:

- Scenario 1: toppling and sliding of rock boulders and debris falls. The sites from which the rock blocks are released are mainly located all along the lower boundary of the unstable B_3 sector.
- Scenario 2: collapse of sector B_3. Continuous rock falls can weaken the rock mass located in this sector. An estimated avalanche involving a rock mass of about $1 \times 10^6\,m^3$ could therefore occur.
- Scenario 3: collapse of the whole B sector. The collapse of sector B_3 could lead to a huge rock avalanche involving the entire B sector, which corresponds to a volume of about $5 \times 10^6\,m^3$.

The occurrence and evolution of each scenario was then analyzed on the basis of geo-mechanical models, in order to assess consequences through the determination of the related hazard.

3.1.1 Geo-mechanical Modeling: Triggering

The site was studied using two geo-mechanical models. The first was a 2D discontinuous model based on the DRAC Finite Element code (Prat et al., 1993) aimed at evaluating the role of discontinuities on the toppling mechanisms, through the simulation of the opening of the interfaces due to the disappearance of the glacier. For more details on these analyses, see Bonnard et al. (2004). The second was a 3D equivalent continuous model carried out by means of MAP^{3D} (Wiles, 2005), a commercial code based on the indirect Boundary Element technique of the Displacement Discontinuity Method. On the basis of the geo-morphological analyses and the 2D numerical results, attention was focused on the lower part of the unstable area (sector B_3), highlighted as the key volume. The aim of the 3D analysis was therefore to simulate the measured displacements in this sector, in order to estimate the mechanical parameters which could trigger such displacements.

The 3D geometrical model was represented as an equivalent continuum, bounded by some discontinuity planes belonging to the principal joint sets and a failure surface corresponding to the shear zone ZT (Fig. 8). The global behavior of this unstable rock volume was then back-analyzed by simulating the mean value of the measured sliding displacements, which were considered to be due to the overall creep behavior of the rock mass, concentrated on the sliding surface.

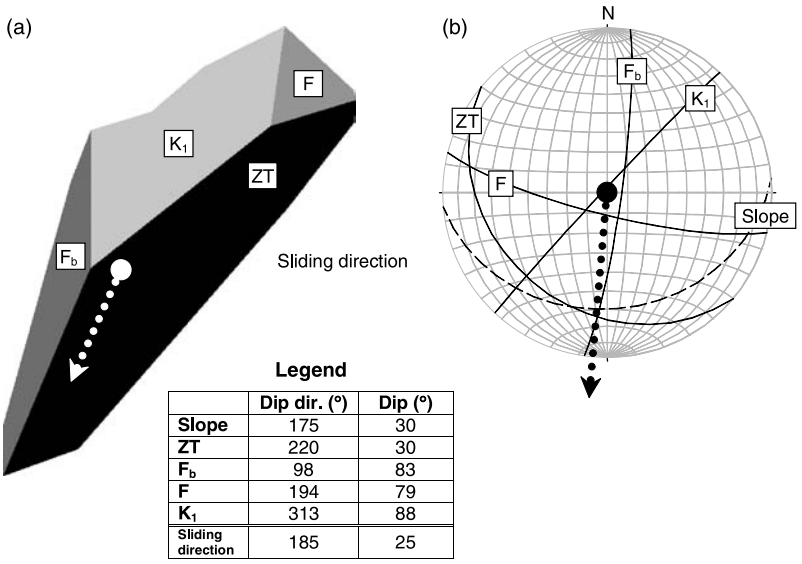

Legend

	Dip dir. (°)	Dip (°)
Slope	175	30
ZT	220	30
F_b	98	83
F	194	79
K_1	313	88
Sliding direction	185	25

Fig. 8. (a) Detaching niche considered in the 3D numerical analyses (sector B_3); (b) kinematic mechanism and sliding direction

Table 2. Mechanical parameters obtained from the 3D numerical model of the Ceppo Morelli landslide

Equivalent continuum			
Unit volume weight	γ	0.027	MN/m^3
Young's modulus	E	7000	MPa
Poisson's ratio	ν	0.25	–
Failure surface			
Friction angle	φ	25	°
Normal modulus	K_n	5000	MPa
Shear modulus	K_s	1500	MPa
Creep coefficient	C	100	MPa · month

Due to the lack of information on the mechanical parameters and the piezometric level, two modeling steps were carried out. In the first, the equivalent friction angle related to the unstable equilibrium conditions of the rock mass was obtained. On the basis of this, the second step was related to the analysis of the behavior of the unstable rock mass with respect to time, and was carried out through a back-analysis of the displacements measured in situ by the monitoring system. No influence on the displacements of the water pressure variations with respect to time was considered. The final set of mechanical parameters obtained from the numerical analyses is given in Table 2.

Even though the creep analyses take into account an implicit time component, it is necessary to note that the results obtained were not able to give the temporal probability of failure needed for the risk analysis, which should be calculated through a probabilistic procedure. For this purpose, however, the variation of pore pressure and the decay of rock strength parameters in time should be known. Since this information was very difficult to obtain because of the many previously described uncertainties, the occurrence probability was derived from a historical analysis, as described in Sect. 3.1.3.

3.1.2 Geo-mechanical Modeling: Run-out

Once the involved volume and the failure mechanisms were established, the run-out phase for the three scenarios was simulated as follows (Bonnard et al., 2004):

Scenario 1 (rock fall)
The trajectories of the falling rock blocks were simulated using the ROTOMAP^{3D} commercial lumped mass code (Geo&Soft, 1999, 2003). Values of the restitution coefficients in the normal and tangential direction equal to 0.32 and 0.80, respectively, and a friction coefficient of 0.65 were assumed. The choice was made on the basis of data obtained from literature and through back-analyses of the trajectories of already fallen rock blocks.

The aim of the analysis was to reproduce the rock falls that had occurred in the past and to simulate new rock falls that could affect a larger area. In order to obtain realistic results, two different source lines were considered, so as to allow the assumed velocity range for the released blocks to be different according to whether they originate from Line 1 (Fig. 9a) or from Line 2 (Fig. 9b) of the considered unstable area. In

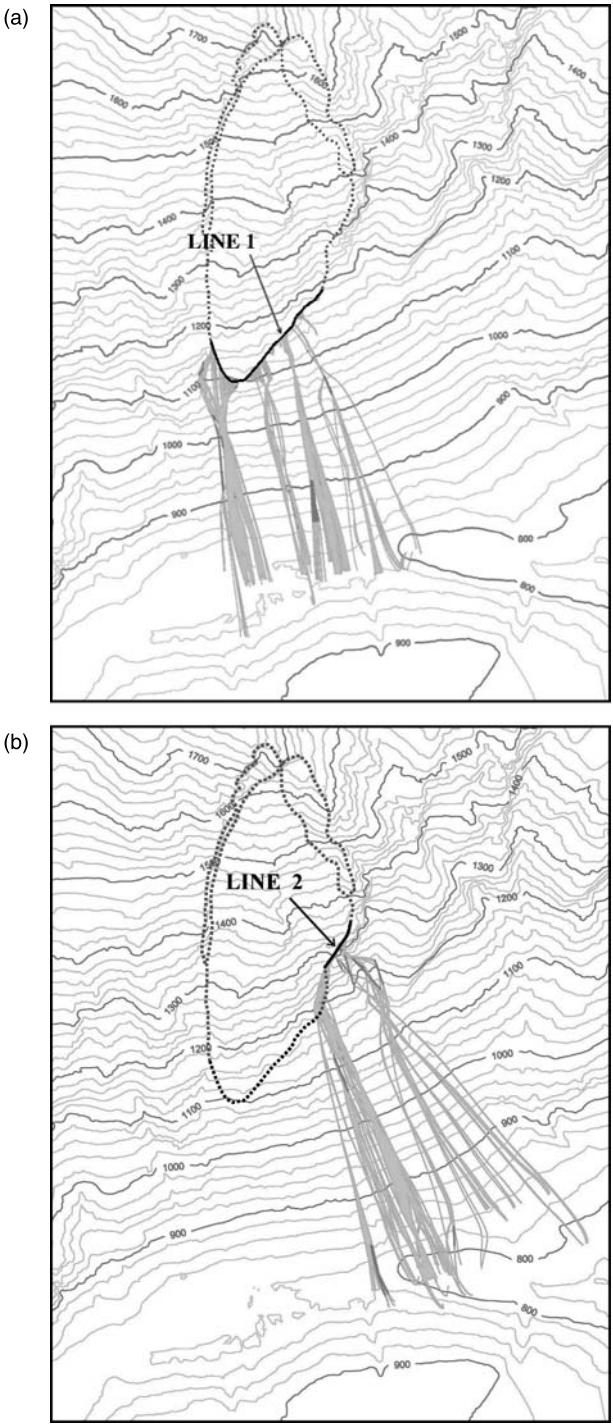

Fig. 9. Scenario 1: rock fall trajectories: a) detachment Line 1; b) detachment Line 2

particular, the velocity from Line 1 was varied from 1 to 1.8 m/s, while the velocity from Line 2 was varied from 0.6 to 1 m/s. These different ranges are justified by the possibility that some of the blocks crossing Line 1 can originate in the upper part of the unstable area and reach a higher velocity. In addition to rock fall trajectories (Fig. 9), the kinetic energy of the blocks was calculated to evaluate the vulnerability of the elements at risk.

Scenario 2 (rock avalanche of about $1 \times 10^6\,m^3$)
The rock avalanche run-out was simulated on the basis of a continuum mechanics approach, through the coupled use of ROTOMAP^{3D} and DAN^{2D}, based on a continuum equivalent analytical method (Hungr, 1995). The DAN code needs to be based on a 2D model, where the width of the run-out area and the avalanche deposit are used as input data; the role of ROTOMAP in this case is therefore to define the lateral extension of the run-out mass as an envelope of the rock fall trajectories. The propagation direction chosen for the DAN^{2D} run-out analyses was the average dip direction of the slope, as shown in Figs. 10 and 11. A frictional rheology, with a friction angle at the base equal to 30° and a pore pressure coefficient equal to 0 (i.e. no water) was assumed in the numerical analyses. Although the avalanche front velocity can be defined by the DAN code along the propagation direction, the vulnerability of the elements at risk was not considered in this case as a function of the process intensity, because a total destruction was assumed in the involved area.

Scenario 3 (rock avalanche of about $5 \times 10^6\,m^3$)
This scenario considers the possibility that the whole volume is involved in a rock avalanche phenomenon. Although extremely unlikely, it was included in the hazard and risk analysis since it could generate particularly catastrophic consequences for the hamlets, the river and the road that are located at the bottom of the valley. The used

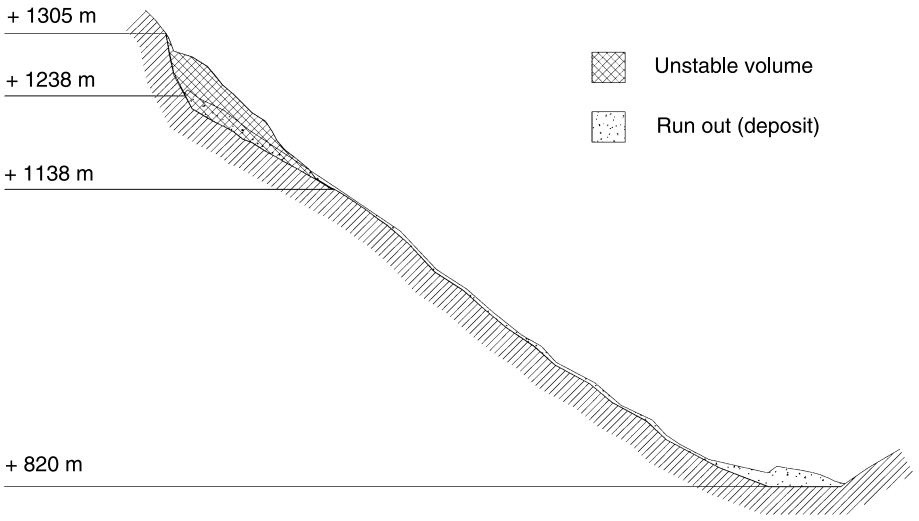

Fig. 10. Section in the propagation direction in the case of scenario 2 (section A–A in Fig. 11)

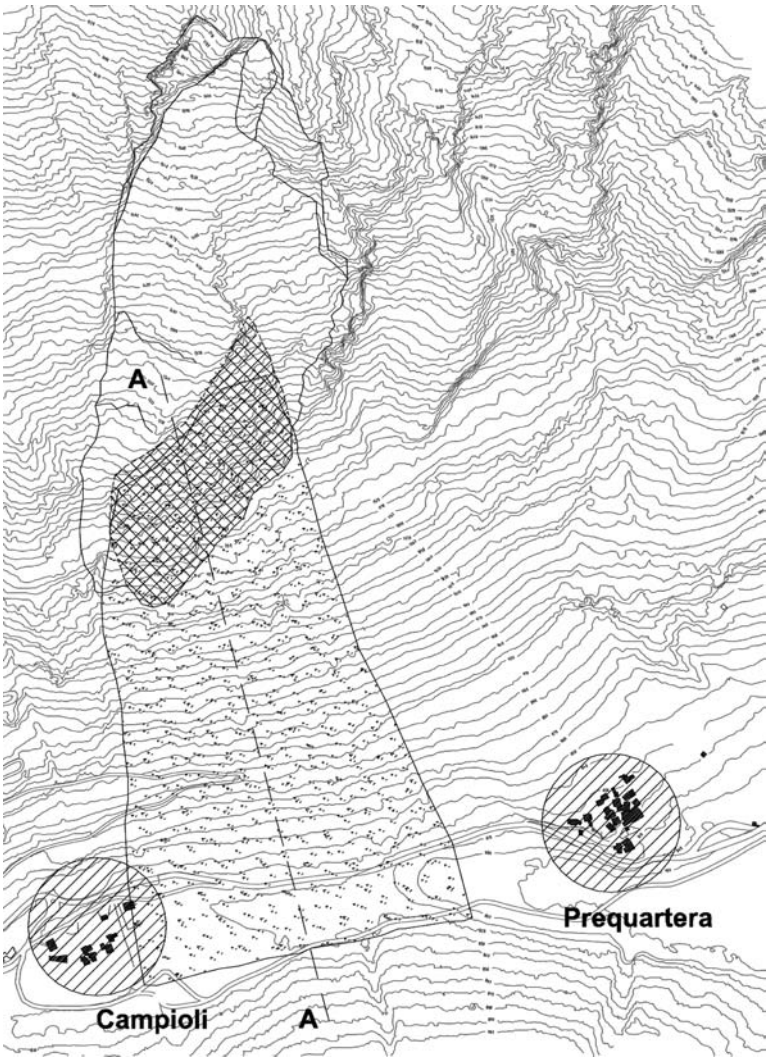

Fig. 11. Run-out area in the case of scenario 2

approach is the same as that of scenario 2 (Figs. 12 and 13), and leads to the determination of the run-out and deposition areas.

3.1.3 Occurrence Probability

Since several records of rock fall activity involving different volumes have existed in the area since the IV century (Regione Piemonte, 2000), a historical approach was adopted to obtain information related to the periodic frequency of different phenomena, leading to some considerations concerning the occurrence probability (for more

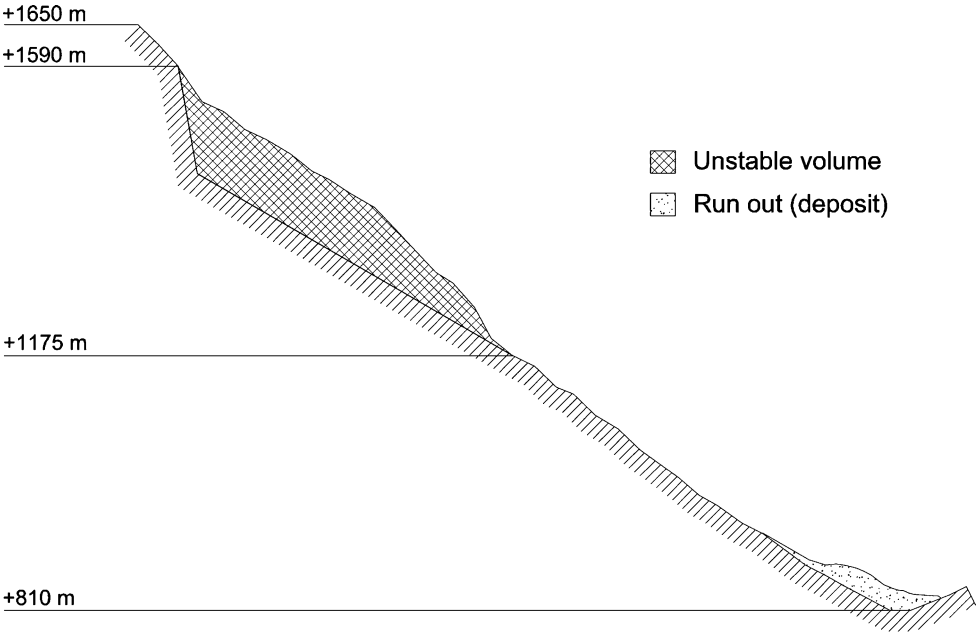

Fig. 12. Section in the propagation direction in the case of scenario 3 (section B–B in Fig. 13)

details, see Bonnard et al., 2004). An occurrence range of time (see also Corominas et al., 2002) was therefore obtained for each of the three evolution scenarios, considering the minimum and maximum time intervals between two consecutive recorded events of different types. A frequency was then calculated, on the basis of their mean value, in terms of events per year (Table 3).

It should be noted that the recorded events are related to only two different types of danger: the fall of non interacting blocks and more severe events involving a larger mass. The first was associated to a rock fall scenario 1 (low energy and high frequency) and the second was considered as being representative of phenomena involving the whole mass, i.e. the rock avalanche corresponding to scenario 3 (high energy and low frequency). It is worth noting that this assumption is very conservative because none of the recorded events appears to have mobilized a volume as large as the whole mass. However, it allows the intermediate occurrence time range to be associated to the rock avalanche scenario 2 (medium energy and frequency), as shown in Table 3.

3.2 Quantitative Risk Analysis

The elements at risk, identified in the GIS environment crossing the involved areas with the available information on land use, include residential areas (historical settlements of Campioli and Prequartera), forest areas, the Auza river, a strategic road (National Road 549), secondary roads, and a very important lifeline (the Valle Anzasca power line).

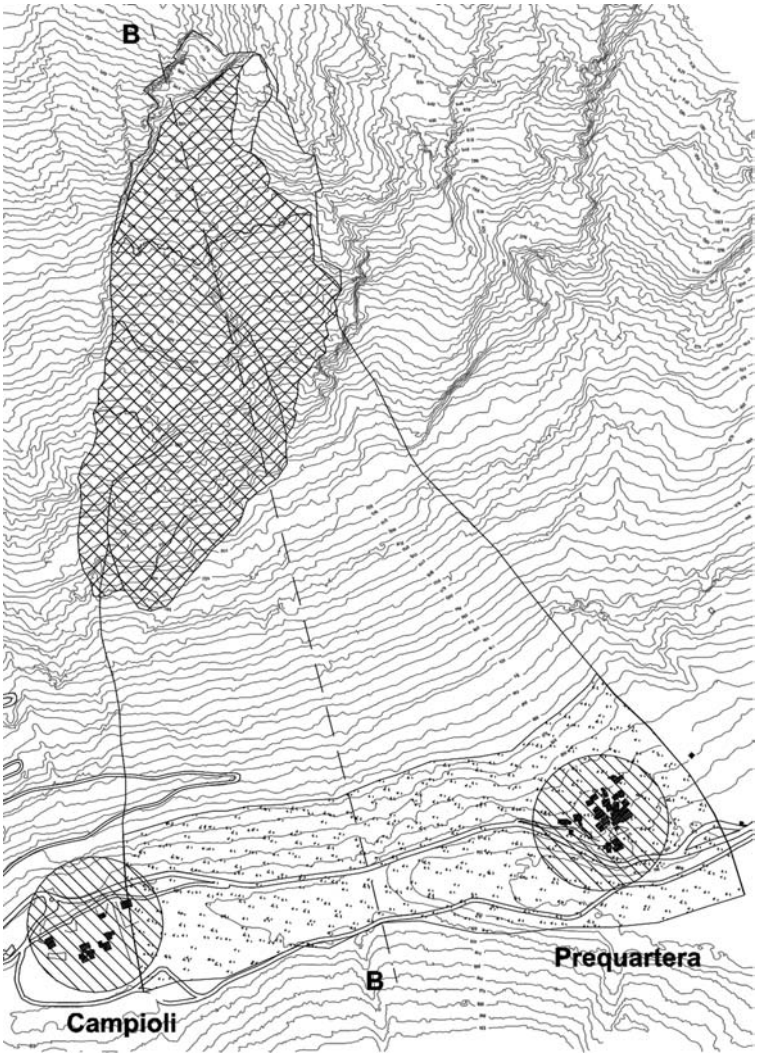

Fig. 13. Run-out area in the case of scenario 3

Three separate risk analyses were carried on, one for each scenario. On the basis of the results different hazard situations were identified for the hamlets located at the bottom of the valley (Figs. 9, 11 and 13). The Prequartera village could be subjected to a rock fall phenomenon (scenario 1) and to the most catastrophic rock avalanche (scenario 3), whereas the expansion of the mobilized mass in both rock avalanche cases (scenarios 2 and 3) could be the cause of a dangerous condition for the Campioli area. The river and the national and secondary roads could be affected by all three scenarios, with different extensions of the involved areas. In particular, an evolution in terms of rock avalanche (scenarios 2 and 3) would determine the interruption of the roads and the damming of the river with disastrous consequences.

Table 3. Definition of the occurrence probability for the Ceppo Morelli landslide using the historical approach

Scenario	Recorded events	Occurrence range (years)	Average (years)	Frequency (occurrence probability) (event/year)
1	1940 Oct. 1971 Apr. 1977 Oct. 2000 Jun. 2002	0–30	15	$1/15 = 0.066$
2	(Intermediate)	30–200	115	$1/115 = 0.009$
3	312 843 1816 2000	200–1000	600	$1/600 = 0.0016$

Different considerations about damage and loss of the elements at risk were obtained for the three scenarios with respect to vulnerability, starting from kinetic energy data obtained by the numerical run-out models. As far as the rock fall scenario (scenario 1) is concerned, different values can be given for the physical, economic, environmental and social vulnerability of the elements at risk (50%, 75% or 100%) as a function of the impact energy (for more details, see Bonnard et al., 2004). On the contrary, in the rock avalanche areas (scenarios 2 and 3), the destruction was considered to be total. Also in the talweg, when the velocity tends to zero, the accumulation (some tens of meters) is so deep that all the assets would be completely destroyed, heavily damaged or buried. According to these considerations, the vulnerability is equal to 100% in all the categories (physical, economic, environmental and social).

In order to obtain the consequences, the vulnerability percentage was multiplied by the values of the elements at risk. In this case, due to the difficulties involved in carrying out detailed economic evaluations (in particular concerning the environmental and social categories), relative value indexes were applied to each category. These indexes do not represent any economic relationship among the elements but only a hierarchical scale of values, as shown in Table 4. The highest social consequences were attributed to residential areas and the strategic National Road 549; the latter also had the highest economic value, as it is the only road to the alpine resort of Macugnaga. From an economic point of view, the Anza stream is also very important because it supplies the Prequartera hydroelectric power plant.

Table 4. Relative values of the elements at risk considered in the Ceppo Morelli case, in a scale ranging from 0 (value nil) to 4 (maximum value)

Element	Physical value	Economic value	Environmental value	Social value
Residential areas	4	1	1	4
Forests	1	1	3	1
Strategic roads	3	4	1	3
Secondary roads	1	2	1	2
Lifelines	1	2	1	0

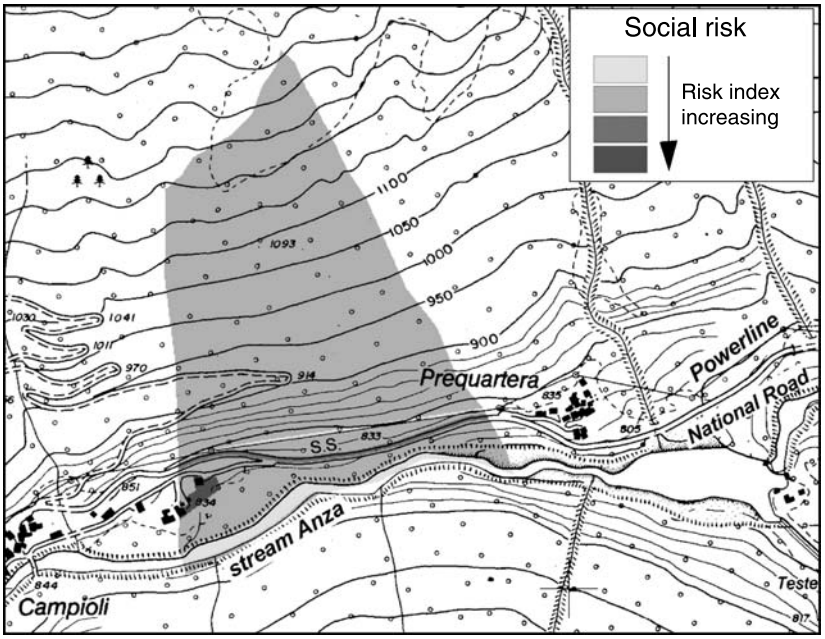

Fig. 14. Social Risk Map obtained from GIS techniques in the case of scenario 2

The last phase of the quantitative risk analysis concerns the risk evaluation. This was obtained by multiplying the consequences by the occurrence probability (P) related to each scenario. Figure 14 shows the results for scenario 2 (vulnerability = 100%; $P = 1/115$ events/year) in terms of social risk, where the areas with different risk degrees for each category are marked. The highest risk values were allocated to the Campioli village and a stretch (0.55 km) of the National Road 549, due to the process type (characterized by a rapid evolution), and the intense traffic of this road in tourist periods.

Finally, the total risks were calculated through a superposition of the three scenarios to obtain a synthesis of the results (see, as an example, Fig. 15, where social risk is again considered). The areas affected by high intensity and high occurrence probability processes present the most elevated risk values. In Ceppo Morelli, the area affected by rock falls shows the highest risk values, as the occurrence probability of this scenario is more than 40 times higher than the occurrence probability of scenario 3 and about 7 times higher than the occurrence probability of scenario 2.

It is necessary to note that, in order to complete the risk analysis, some considerations about the indirect effects associated to the landslide evolution (not considered by the geo-mechanical models) should be made. In particular, the formation of a landslide dam lake should be considered because it could generate a large basin in a few hours, causing the inundation of many buildings in Campioli. Moreover, a flash-flood along the valley due to instantaneous lake depletion could cause problems to the downstream villages, and greatly extend the involved areas. A qualitative study was carried out in Ceppo Morelli to obtain details concerning

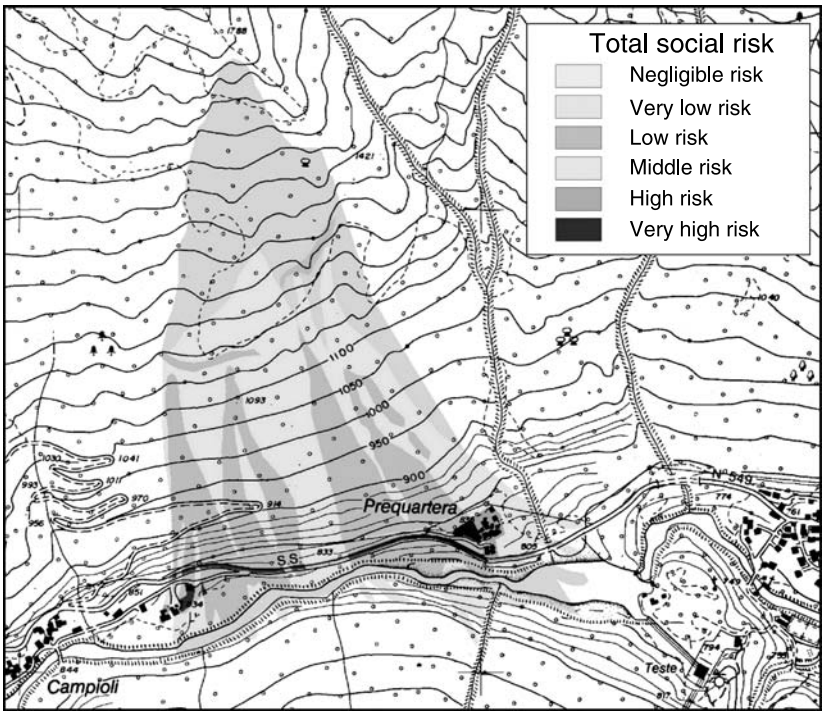

Fig. 15. Example of a total risk assessment for the social category

the planning of civil protection works in the case of flash-flood events (Bossalini and Cattin, 2002).

4. The Rosone Landslide

The entire southern side of the ridge bounded by the Orco and Piantonetto rivers, in the Province of Turin (Italy), has been undergoing a slow deep-seated gravitational slope deformation process for many years. The landslide movement is historically known as the *Rosone landslide* because it frequently involved the small village of Rosone, which was in the past located at the toe of the slope and then relocated outside the affected area during the fifties. At present, this phenomenon also involves the Electricity Agency (AEM) of the city of Turin hydroelectric power plant and National Road 460 which are located at the toe of the slope. The Rosone landslide involves an area of about 5.5 km^2 and reaches a depth of several decameters (Ramasco et al., 1989). It affects a 1300 m high slope, from an altitude of 2000 m at the ridge crest down to 700 m at the bottom of the valley (Fig. 16).

4.1 Danger Identification and Hazard Analysis

The morphological and structural characteristics of the area suggest its subdivision into three adjacent sectors, roughly corresponding to the villages of Ronchi, Perebella, and

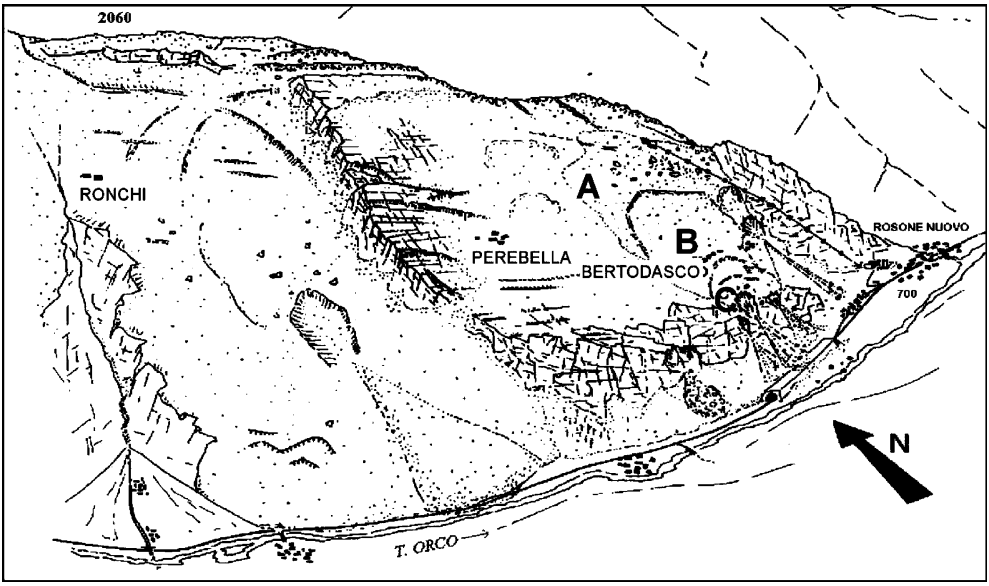

Fig. 16. Sketch of the Rosone landslide (Brovero et al., 1996)

Bertodasco (Fig. 16). These sectors reflect the final, early, and intermediate stages of the evolution of the deep-seated gravitational process respectively. Examining the area from west to east, the Ronchi sector is encountered first and it is characterized by a highly advanced stage of evolution which caused the disruption of the original rock mass. This sector can now be assumed to be substantially stable. The central sector, around Perebella, reflects an early stage in the deformation process. It is clearly separated from the Ronchi sector by a NS striking scarp a few hundred meters long and 50–90 m high. The bedrock is more damaged in the middle and lower parts of this sector. The eastern sector (Bertodasco), which hosts the AEM electric power plant, shows an intermediate deformation stage between those of the Ronchi and Perebella sectors.

Previous studies (Forlati et al., 1993) identified the Bertodasco sector as the one most likely to undergo a catastrophic evolution. A morpho-structural analysis revealed the presence of three zones with different degrees of mobility, from the top to the toe of the valley, referred to as A, B and C (Fig. 17):

a) Zone A includes the upper part of the Bertodasco sector, where the movements of the slope and related morphological evidence are poorly defined. Although disrupted, this zone still preserves its original structural features. This suggests the presence of minor translational movements, which have been confirmed by the monitoring system located in the Bertodasco sector by AEM (Forlati et al., 1993). The eastern lower part of zone A shows more prominent movements, which are indicated by open fractures, and it is affected by undulations and local bulges. The rock mass is here subdivided into blocks, although it is still aligned along the main joint systems.

b) Zone B is bounded by a prominent curved scarp and by rectilinear scarps subparallel to the main joint systems. These scarps often act (at least since 1953) as

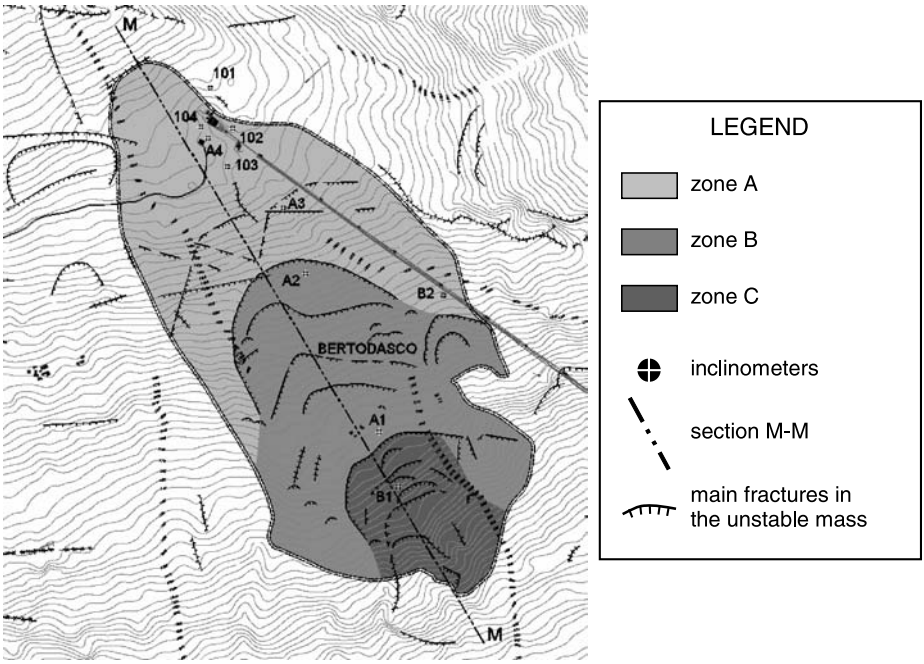

Fig. 17. Morpho-structural map of the Bertodasco sector, showing the subdivision into distinct morphological zones A, B and C (see also section M–M in Fig. 19), the main discontinuities and the location of the inclinometers

tension cracks that have opened due to the displacements that occurred along the schistosity. These kinematics are closely related to the shape and orientation of the rock blocks that result from the intersection of natural joint systems (see Fig. 18). The gravitational instability of zone B has also induced a partial translation of the eastern lower part of zone A, and caused the displacement of the AEM power plant pipes. Toppling and rolling of rock blocks have been observed at the eastern boundary of zones A and B. These rock blocks frequently moved towards the ancient Rosone village and as a consequence the new Rosone village (Rosone Nuovo) was constructed in a new location.

c) Zone C consists of a very heterogeneous mobilized mass which has been affected by major gravitational movements since the 1930s. It consists of disengaged rock blocks of different sizes; a mixture of chaotic coarse gravel and fine material. The movements mainly affect the upper part of the zone along many concave and subparallel scarps characterized by offsets of 1–10 m. Over the last fifty years, the movements in the upper part of this zone have caused the destruction of part of the Bertodasco village, which has now been completely abandoned. The lower part of zone C is instead affected by rock-debris and debris flows that in the past destroyed National Road 460 along the Orco valley.

The danger characterization was only focused on the Bertodasco sector due to the peculiar hazard conditions and the availability of monitoring data recorded by AEM.

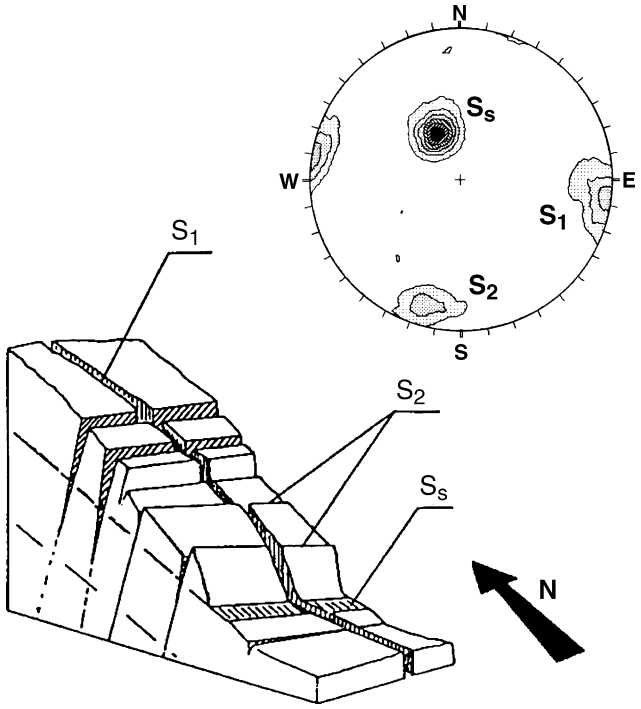

Fig. 18. 3D sketch of the main tectonic discontinuities of the Rosone area. The joint systems poles and the schistosity are shown on a Schmidt diagram

In particular, two zones with major movements were considered: zone B, mainly characterized by planar sliding surfaces, and zone C, where rotational sliding is inferred. The main structural elements that were considered for the hazard analysis (Figs. 17 and 18) are:

- the schistosity S_S, with a mean dip direction of 154° and a dip of 34°;
- the sub-vertical joint systems S_1, with a mean dip direction of 277° (100°) and a dip of 80° (85°);
- the sub-vertical joint systems S_2, with a mean dip direction of 203° (15°) and a dip of 86° (68°);
- an inferred deep (about 40–75 m) failure zone (shear band) at the base of the Bertodasco sector (zones B and C), considered to be sub-parallel to the schistosity.

The presence and geometry of this inferred surface was highlighted by the results of the inclinometer measurements and geophysical investigations carried out in the landslide area (Fig. 19 and Table 5).

The rock slope toe, over deepened by glacial erosion and weakened by severe stress concentrations, is not very likely to be able to prevent a global movement of the slope. As the deformation that affects the middle part of the slope could spread through the basal part, a quite defined failure surface might be formed, leading to a huge landslide (rock avalanche). Three different evolution scenarios have been

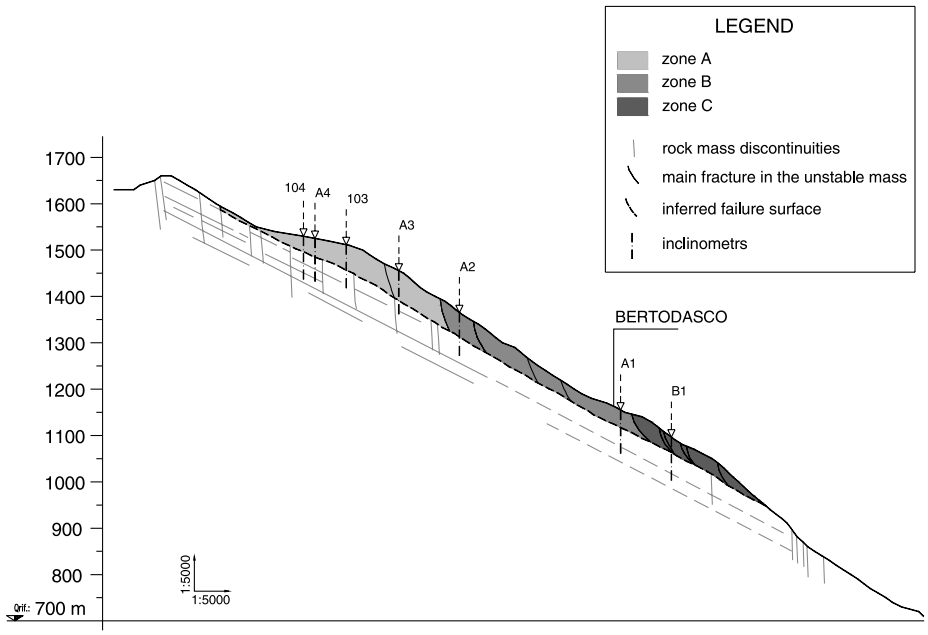

Fig. 19. Cross-section of the Rosone landslide (section M–M in Fig. 17) and location of the inclinometers. The shape of the sliding surface was derived from the inclinometer measurements

Table 5. Inclinometric measurements in the Rosone landslide (see Fig. 17 for the instrument positions)

	Measurement period		Failure surface depth [m]	Surface displacements		
	Initial	Last		[mm]	Annual average [mm/year]	Dip direction [°]
A1	12/12/1991	3/6/1999	38.98	157.1	21.00	187.9
A2	12/12/1991	9/11/2000	45.72	131	14.69	170.1
A3	12/12/1991	5/10/1993	71.31	closed	–	–
A4	12/12/1991	6/11/2002	30.00	73.4	6.73	158.7
101	6/12/1984	27/11/1993	3.05	57.7	6.42	147.9
102	6/12/1984	6/11/2002	22.55	116.3	6.49	157.1
103	6/12/1984	7/11/2000	52.42	117.1	7.35	165.5
104	6/12/1984	7/11/2000	20.12	89.5	5.62	149.3
B1	17/11/1999	25/10/2000	40.23	131.5	–	144.3
B2	17/11/1999	6/11/2002	37.78	56.2	18.91	162.7

taken into account, with decreasing occurrence probability and increasing impact on land planning:

- Scenario 1: collapse of zone C (Fig. 17). The rock mass of zone C is heavily fractured, continuous rock falls could therefore weaken the rock mass located in this sector. An avalanche involving a rock mass of about $2.2 \times 10^6\,m^3$ could then occur.
- Scenario 2: collapse of zones C and B (Fig. 17). The total volume involved would be about $9.3 \times 10^6\,m^3$.

• Scenario 3: collapse of the whole landslide area (A + B + C, Fig. 17), involving a volume of about $20.5 \times 10^6\,m^3$. In zone A, the quality of the rock body, which is much less fractured than the other zones, and the recorded displacements, which are lower than those recorded in zones B and C, suggest that this scenario should be considered less probable than the previous ones.

4.1.1 Geo-mechanical Modeling: Triggering

As for Ceppo Morelli, 3D numerical analyses have been carried out by using the MAP^{3D} commercial code, based on the indirect Boundary Element technique of the Displacement Discontinuity Method. The aim of the 3D analyses, focused on zones B and C, was to estimate the mechanical parameters of the rock mass through the back-analysis of the monitored displacements. The simplification introduced into the numerical analyses are the same as for Ceppo Morelli: the 3D geometrical model was represented as an equivalent continuum, separated from the rest of the slope by the sliding surface and some discontinuity planes belonging to the main joint sets. The mean value of the measured sliding displacements was simulated as being due to the overall creep behavior of the rock mass, which was assumed to be concentrated on the sliding surface. No influence on the displacements due to water pressure variations with respect to time was considered.

Due to the lack of information on the mechanical parameters and their evolution versus time, the same two-step numerical procedure was used as for Ceppo Morelli. The search for the mechanical parameters related to the unstable equilibrium conditions of the rock mass was performed in the first one. On the basis of the obtained results, the analysis of the behavior of the unstable rock mass with respect to time was developed in the second step through back-analyses of the in-situ displacements.

Since, in this case, the definition of the failure surface through the geological models is affected by many uncertainties, a preliminary definition of the geometrical constrains

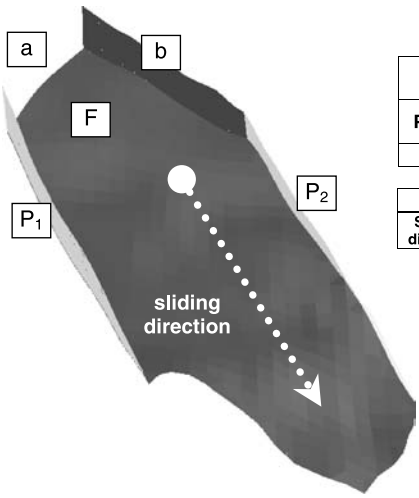

Legend

a, b	open vertical tensile joints (see figure 19)
P_1, P_2	planes belonging to system S_1 (see figure 18)
F	failure surface

	Dip dir. (°)	Dip (°)
Sliding direction	185	25

Fig. 20. The detaching niche considered in the 3D numerical analyses (zones B and C, Bertodasco sector)

Table 6. Mechanical parameters obtained from the numerical triggering analysis for the Rosone landslide

Equivalent continuum			
Unit weight	γ	0.027	MN/m^3
Young's modulus	E	7000	MPa
Poisson's ratio	ν	0.25	–
Failure surface			
Friction angle	φ	25	°
Normal modulus	K_n	5000	MPa
Shear modulus	K_s	1500	MPa
Creep coefficient	C	170	MPa · year

of the landslide was obtained through the Digital Elevation Model (DEM) of the Orco Valley and the available data derived from geophysical analyses and geotechnical site investigations. The position and shape of the failure zone was obtained by means of an interpolation methodology. The estimated rock volume delimited by such a failure surface, the topographic surface and the sub-vertical joints assumed as boundaries of zones C and B is about $11 \times 10^6\,m^3$, which is in good agreement with the estimation made on the basis of the geo-morphological studies. The 3D representation of the detaching niche, obtained as previously described, is shown in Fig. 20.

The final set of the mechanical parameters obtained through the back-analyses is shown in Table 6. Such results seem to confirm the consistency between the measured displacements and the kinematical considerations made on the basis of the geological studies. The same considerations as in the case of Ceppo Morelli apply as far as the meaning of such results and the determination of the occurrence probability are concerned.

4.1.2 Geo-mechanical Modeling: Run-out

The three previously described scenarios were analyzed by Enel. Hydro (De Lotto and Moia, 2001) through the application of an empirical methodology due to Friz and Pinelli (1993), based on both mechanical and statistical considerations. A detailed description of the methodology can be found in De Lotto and Moia (2001) and Bonnard et al. (2004). Only the main results are summarized in this paper (Table 7), in terms of maximum axial sliding distance of the landslide along the slope (Ra) and maximum lateral expansion of the accumulation in the bottom of the valley (Sl).

Table 7. Maximum axial sliding distance and lateral expansion values obtained through the Friz and Pinelli (1993) methodology on the Rosone landslide

Scenario	Maximum axial travel distance Ra (m)	Maximum lateral expansion Sl (m)
1 (Sector C)	949	671
2 (Sectors C + B)	1438	1315
3 (Sectors C + B + A)	1910	1619

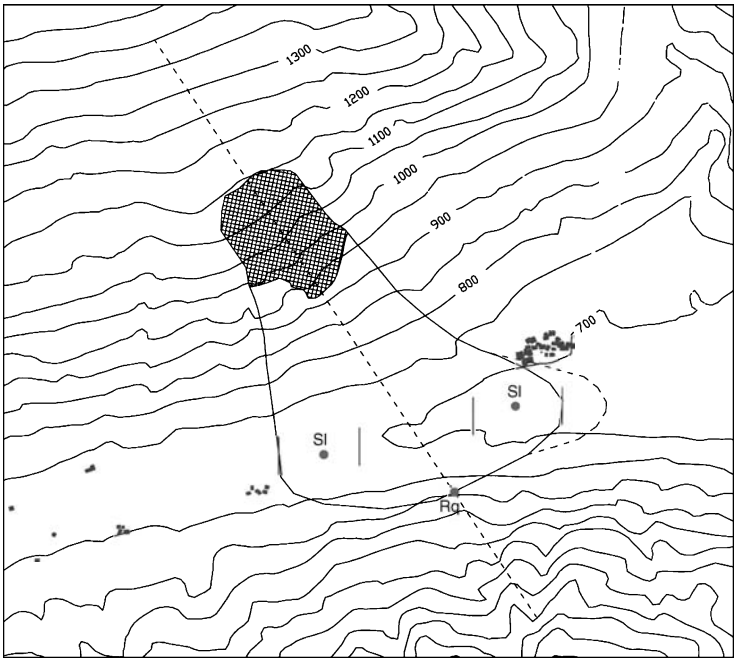

Fig. 21. Result obtained through the Friz and Pinelli (1993) methodology in the case of scenario 1

In order to define the maximum axial sliding distance Ra, the unstable mass was considered as a dimensionless block that slides on an assigned topography and which is subjected to gravity and basal resisting forces (Perla et al., 1980). The mechanical characteristics were considered to be constant and their value was defined through the back-analysis of a large number of historical cases. Instead, the maximum lateral expansion Sl was statistically defined on the basis of a large number of historical cases. The shape of the possible run-out area was obtained through a graphical interpretation of the topography, as shown in Fig. 21 with reference to scenario 1. The continuous line in the figure represents the Ra and Sl values under the hypothesis that the run-out area is symmetrical to the axial sliding distance, while the dashed line considers the hypothesis of a prevalent expansion of the mass in the direction of the valley. The volume of the accumulation is considered to be 1.3 times the initial unstable volume.

In order to integrate the Enel.Hydro results, the rock avalanche run-out in the case of scenario 1 was simulated by applying the DAN^{2D} code (Hungr, 1995). The geometry of the considered unstable mass is approximately the same as that assumed by Enel. Hydro. A frictional rheology was assumed for the whole path and the possibility of material entrainment during the run-out was simulated by increasing the volume of a prescribed amount, in proportion to the sliding distance.

The results obtained by Enel.Hydro were then back-analyzed to calibrate the friction angle and volume change rate. Considering a unit volume weight $\gamma = 26.50\,\mathrm{kN/m^3}$ and a pore pressure coefficient $= 0$, the best results were obtained with a friction angle of 19.7° and a volume change rate of about $730\,\mathrm{m^3/m}$. The main output data obtained

Table 8. DAN output data for the Rosone landslide

Run-out time [s]	61.40
Maximum front velocity [m/s]	46.57
Maximum depth of the accumulation [m]	31.82
Involved volume [m^3]	
Initial	1856058.38
Final	2428449.50

using these parameters are shown in Table 8. It should be emphasized that the friction angle obtained from the back-analysis, although very low for a rock mass, should be considered as being representative of all the factors statistically taken into account in the Fritz and Pinelli methodology, such as the presence of water, gouge material on the sliding surface, etc.

The application of the DAN^{2D} code led to an improvement in the knowledge of the mass behavior during the propagation and the accumulation phases. The obtained data were not only the run-out distance and the run-up on the opposite slope but also the landslide velocity, the time of propagation, and the extension and the depth of the accumulated mass once it stops. The analyses carried out underline that, in the case of a catastrophic evolution (scenarios 2 and 3), the landslide would determine the damming of the river with disastrous indirect consequences.

4.1.3 Occurrence Probability

As in the case of Ceppo Morelli, quantitative methods could not be applied to determine a temporal probability of failure, because the uncertainty in the definition of the parameters involved was too large and it was not possible to define any reliable variability for them. Since several historical records exist on the landslide activity in the area involving different volumes, the historical approach seemed much more suitable to obtain some information related to periodic frequency.

A frequency of less than 10 years was found for both rock fall/debris flow phenomena and the Bertodasco sector (zone C) instability (scenario 1) from an analysis of the historical data. This indicates a relationship among these phenomena: the movements in zone C caused the block fall from the scarp over National Road 460. This situation is particularly noticeable during heavy rainfall. On the other hand, the instability of zones B + C (scenario 2) is characterized by a recorded phenomena frequency of between 0 and 30 years, while the whole slope (zones A + B + C) showed important movements (scenario 3) during the year 1953 and probably at the beginning of the XVIII century, with an interval of about 250 years. It should be noted that these sectors are subjected to deformations, which are almost continuous in time. Under particular conditions, they accelerate, leaving morphological evidence on the slope and sometimes provoking damage. The recorded historical data and the temporal intervals of the occurrence probability refer to these paroxystic phases; the next ones could cause sudden collapses of the slope with the development of rock avalanche phenomena.

An occurrence time range was obtained for each scenario, considering the minimum and maximum time intervals between two consecutive recorded events. A frequency was then calculated on the basis of their mean values, in terms of events per year (Table 9).

Table 9. Temporal frequency calculated in terms of events per year for the Rosone landslide

Scenario	Occurrence range [years]	Average [years]	Frequency (occurrence probability) [event/year]
Rockfall & debris flow	$0 \div 50$	25	$1/25 = 0.04$
1. Rock avalanche (zone C)	$0 \div 50$	25	$1/25 = 0.04$
2. Rock avalanche (zones B + C)	$50 \div 250$	150	$1/150 = 0.007$
3. Rock avalanche (zones A + B + C)	>250	1000	$1/1000 = 0.001$

4.2 Quantitative Risk Analysis

The Quantitative Risk Assessment was carried out with reference to the three rock avalanche scenarios, focusing on the Bertodasco sector.

The elements at risk were identified in the GIS environment, crossing the involved areas with the available information on land use, and include residential areas (the Rosone village and minor small settlements), forest areas, one strategic road (National Road 460), secondary roads, and a very important lifeline (Power line "Valle Locana"). As in the case of Ceppo Morelli, the value of the elements at risk was defined on the basis of relative indices referring to each category, as detailed in Table 4.

Since the destruction can be considered total in the whole affected areas of the rock avalanche scenarios, a distinction between various degrees of energy based on landslide velocity would have been useless to define the vulnerability of the elements at risk, which was therefore set equal to 100% for all the categories (physical, social, economic and environmental).

Risk maps were then obtained with reference to each category and for each scenario. Total risk maps were also defined for each category by adding the risk values obtained in the three scenarios, as shown in Fig. 22 with reference to the physical risk. The map in Fig. 22 underlines the areas with the highest risk value, i.e. National Road 460 and part of the new Rosone village. Moreover, part of the accumulation would involve the hydro-electric power plant and part of the failure area would involve the penstocks. In this case, the total risk level is low because these elements are only affected by scenario 3. The map in fact emphasizes that the risk is closely linked to the occurrence probability.

In order to complete the risk analysis, some considerations concerning the indirect effects linked to rock avalanche were made on the basis of descriptive and qualitative evaluations derived from case histories (i.e. Hsü, 1975). The large mass movement that could occur in Rosone would produce a huge wind effect. The intensity of the processes are not easy to calculate but it is probable that they would be light laterally to the mass movement and very strong frontally. The same would occur for the dust that follows the wind effect.

Another effect that should be considered in risk assessment is the formation of a landslide dam lake. This phenomenon could occur during a meteorological event with important flows along the Orco river (some hundreds m^3/s) and would form a basin of some thousand m^2 in a few hours. Many buildings would be inundated and many people would have to be evacuated, thus increasing the social risk.

Finally, due to lake formation, the downstream villages could be involved but, although flash-flooding along the valley could cause enormous problems, its effects have not yet been analyzed.

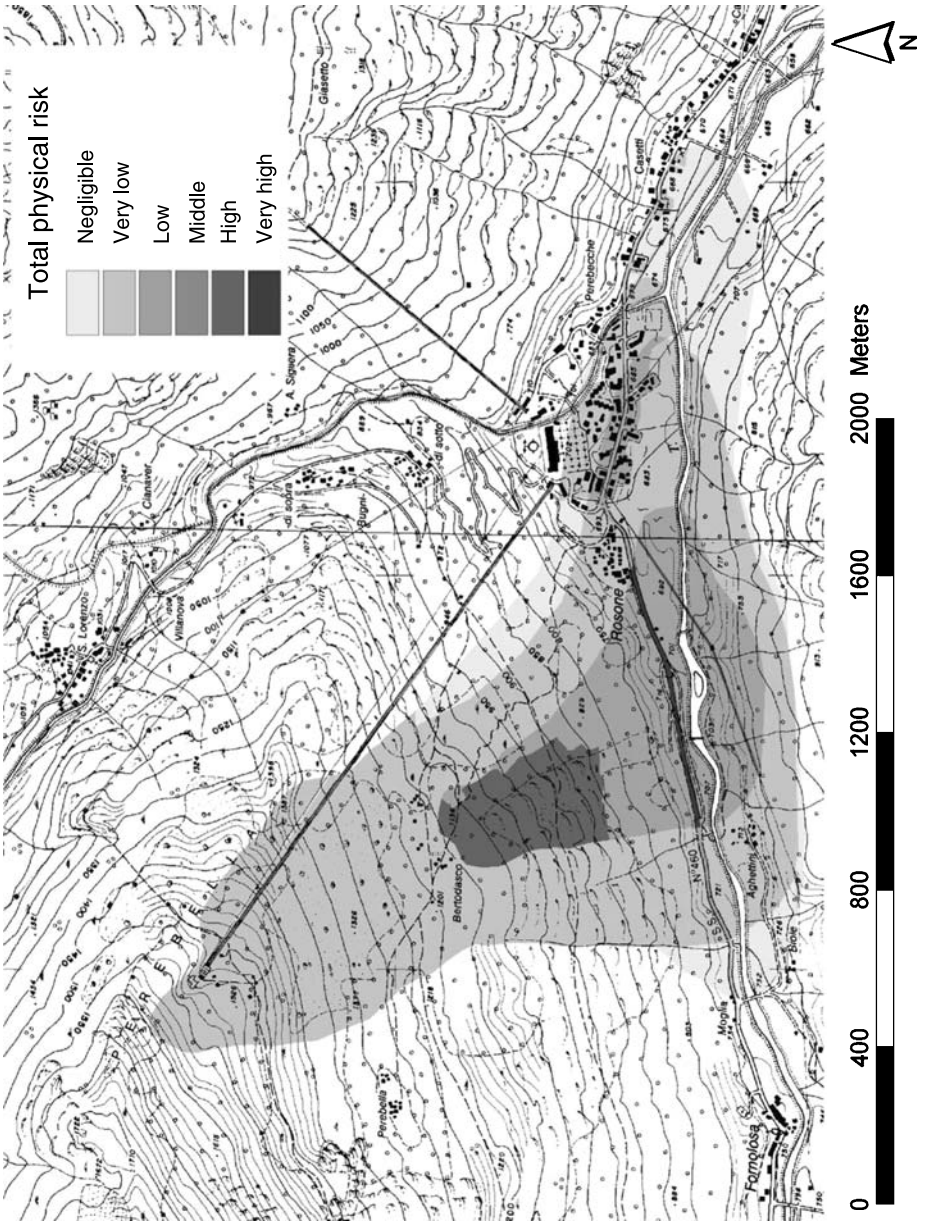

Fig. 22. Total physical risk map obtained by GIS

5. Conclusions

The multidisciplinary hazard and risk analysis methodology developed as part of the IMIRILAND project for large landslides that could evolve into catastrophic rock avalanches has been presented in this paper and exemplified through its application to the Ceppo Morelli and Rosone sites, located in the Italian Western Alps.

The results show that the definition of a hazard is extremely uncertain in the case of large landslides because it requires important simplifications of the reality and the necessity of assuming some parameters which cannot be directly measured. This analysis is therefore difficult despite the use of sophisticated numerical techniques, the amount of available data and the reliability of geological models.

Indeed, scientific knowledge is still far from being able to accurately predict the failure of a landslide in a quantitative manner, even though the mechanics of the processes involved are fairly well known. This is particularly true for the prediction of the temporal probability of occurrence, which is closely linked to the variation in time of the mechanical characteristics and the boundary conditions.

As described in the paper for the Ceppo Morelli and Rosone landslides, due to the limited understanding of the mechanical behavior of the involved materials and the lack of monitoring data, occurrence probability can only be computed in many cases through a historical analysis of past events, linked to geo-morphological considerations with reference to different time periods.

The sequential quantitative risk assessment methodology proposed in this paper is based on the development of integrated phases, each one being independent of the approach used in the previous step. Thus, despite the previously described limitations, the methodology is robust even though it leads to final results in terms of consequences and risks which depend on the quality and reliability of the input data. This allows the obtained results to be easily improved if a more reliable quantification of the process intensity, the involved areas and the occurrence probability could be carried out in the future, on the basis of the acquisition of new data and knowledge.

Acknowledgements

The IMIRILAND, *Impact of Large Landslides in the Mountain Environment: Identification and Mitigation of Risk*, project has been supported by the European Union as part of the 5th Framework Programme (contract EVG1-CT-2000-00035). The Authors wish to thank all the partners involved in the project for their contribution to the work presented in this paper.

References

Berggren, B., Berglund, C. (eds.) (2000): Concerted action for forecasting, prevention and reduction of landslides and avalanche risk (CALAR). Final Report, Swedish Geotechnical Institute, Linköping, Sweden.

Bonnard, C., Forlati, F., Scavia, C. (eds.) (2004): Risk analysis of large landslides in alpine environment: the IMIRILAND project. Rotterdam, Balkema.

Bossalini, G., Cattin, C. (2002): Studio dell'onda di piena conseguente ad una ipotetica frana in località Prequartera. Internal report, Regione Piemonte, Comunità montana Valle Anzasca (in Italian).

Brovero, M., Campus, S., Forlati, F., Ramasco, M., Susella, G. (1996): La frana di Rosone, Valle Orco. In: J. Fourier (ed.), Regione Piemonte & Universitè I. Fourier (eds.), Rischi Generati da Grandi Movimenti Franosi, Programme Interreg I Italy-France, 143–177 (in Italian).

Canuti, P., Casagli, N. (1994): Considerazioni sulla valutazione del rischio di frana. Proc. of ''Convegno Fenomeni Franosi e Centri Abitati'' Regione Emilia Romagna, CNR-GNDC, Bologna, 1–58 (in Italian).

Castelli, M., Forlati, F., Scavia, C. (2001): Landslides: the questions of the decision-maker and the answer of the modelisation. Proc. 1st Int. Conf. Albert Caquot, Paris, October 2001.

Cherubini, C., Giasi, C. I., Guadagno, F. M. (1993): Probabilistic approaches of slope stability in a typical geo-morphological setting of southern Italy. Risk and reliability in ground engineering. Thomas Telford, London, 144–150.

Corominas, J., Copons, R., Vilaplana, J. M., Altimir, J., Amigò, J. (2002): Integrated landslide susceptibility analysis and hazard assessment in the principality of Andorra. Nat. Hazards 30(3), 421–435.

Cruden, D., Fell, R. (eds.) (1997): Landslide risk assessment. Proc. Int. Workshop, Honolulu, 19–21 February, 1997. Rotterdam, Balkema.

De Lotto, P., Moia, F. (2001): Attività di progettazione ed installazione di un sistema di monitoraggio integrato del movimento franoso di Rosone (TO); scenari di rischio. Prog. ISMES 2338, Internal Report, Settore Studi e Ricerche Geologiche ARPA Piemonte (in Italian).

Einstein, H. H. (1988): Landslide risk assessment procedure. Special Lecture, Proc. 5th Int. Symp. on Landslides. Lausanne, Switzerland, Rotterdam, Balkema, 2, 1075–1090.

Forlati, F., Ramasco, M., Susella, G., Barla, G., Marino, M., Mortara, G. (1993): La deformazione gravitativi di Rosone: un approccio conoscitivo per la definizione di una metodologia di studio. Studi Trentini di Scienze Naturali, Acta Geologica. 68, 71–108 (in Italian).

Friz, E., Pinelli, P. F. (1993): Ricerche sull'area di invasione di valanghe di roccia. Proc. National congress ''Fenomeni Franosi'', Riva del Garda, Italy. Studi Trentini di Scienze Naturali, Acta Geologica. 68, 55–65 (in Italian).

Geo&Soft International (1999): ROTOMAP for Windows. Torino, Italia.

Geo&Soft International (2003): ISOMAP & ROTOMAP for Windows (3D surface modelling & rock fall analysis). User's guide, Torino, Italia.

Hsü, K. J. (1975): Catastrophic debris streams (sturzstroms) generated by rock falls. Geol. Soc. Am. Bull. 86, 129–140.

Hungr, O. (1995): A model for the run-out analysis of rapid flow slides, debris flows, and avalanches. Can. Geotech. J. 32, 610–623.

Mayoraz, F., Cornu, T. H., Djukic, D., Vuillet, L. (1997): Neural networks: a tool for prediction of slope movements. Proc. 14th Int. Conf. on Soil Mech. and Foundation Eng., Hamburg, 1, 703–706.

Morelli, M., Piana, F., Polino, R. (2003): Integrated remote sensing and field structural analyses on large landslide in NW Alps – the IMIRILAND project approach. GeoItalia 2003, 4th Italian Forum on Earth Science, Abstract.

Perla, R., Cheng, T., McClung, D. (1980): A two-parameter model of snow-avalanche motion. J. Glaciol. 26(94), 197–207.

Pirulli, M. (2005): Numerical modelling of landslide runout. Doctoral thesis, Politecnico di Torino, Dipartimento di Ingegneria Strutturale e Geotecnica (supervisor: Prof. Claudio Scavia).

Prat, P., Gens, A., Carol, I., Ledesma, A., Gili, J. A. (1993): DRAC: a computer software for the analysis of rock mechanics problems. In: Liu (ed.), Application of computer methods in rock mechanics. Shaanxi Science and Technology Press, Xian, China, 1361–1368.

Ramasco, M., Stoppa, T., Susella, G. (1989): La deformazione gravitativa profonda di Rosone in Valle Orco. Boll. Soc. Geol. It. 108, 401–408 (in Italian).

Regione Piemonte (2000): La frana di Prequartera, analisi del movimento franoso e valutazione delle potenziali fasi evolutive e schema del sistema di controllo del fenomeno franoso. Internal Report (in Italian).

Varnes, D. J. (1984): Landslide hazard zonation: a review of principles and practice. Natural Hazard, 3, Paris, France. UNESCO, 63 pp.

Vengeon, J. M., Hantz, D., Dussage, C. (2001): Prédictibilité des éboulements rocheux: approche probabiliste par combinaison d'études historique et géoméchanique. Revue Française de Géotechnique 95/96, 143–154 (in French).

Wiles, T. D. (2005): Map3D user's manual, Mine modelling (Pty) report, www.map3d.com.

Author's address: Marta Castelli, Politecnico di Torino – Dipartimento di Ingegneria Strutturale e Geotecnica, Corso Duca degli Abruzzi 24, 10129 Torino, Italy; e-mail: marta.castelli@polito.it